Int. J. Nano Dimens., 8 (2): 97-106, Spring 2017

ORIGINAL ARTICLE

Some studies on the surface modification of sol-gel derived hydrophilic Silica nanoparticles

Tayseir Mohammed Abd Ellateif [1, 2, *]; *Saikat Maitra* [3]

[1]*Chemical Engineering Department, Universiti Teknologi PETRONAS, Tronoh-31750, Perak, Malaysia*
[2]*Gas Processing Center, College of Engineering, Qatar University-2713, Doha, Qatar*
[3]*Government College of Engineering and Ceramic Technology, Kolkata-700010, India*

Received 27 December 2016; revised 18 February 2017; accepted 07 March 2017; available online 14 March 2017

Abstract

In the present investigation surface modification of silica nanoparticles by alumina was carried out by sol-gel process. Fourier transform infrared (FTIR) and X-ray fluorescence (XRF) confirmed the synthesis of silica and the surface modification as alumina is anchored to silica surface. Field emission scanning electron microscopy (FESEM) and transmission electron microscopy (TEM) investigations observed that alumina doping affected significantly the morphology, particle size distribution and surface area of the synthesized nanoparticles. From N_2 adsorption-desorption isotherms studies it was further noted that alumina doping improved the pore volumes of the synthesized silica nanoparticles and the synthesized silica alumina nanoparticles are mesoporous materials. The hydrophobicity test and thermal stability results confirmed the modification and conversion of silica to hydrophobic materials using alumina.

Keywords: *Alumina; Nanoparticles; Pore size; Silica; Sol-gel method*

How to cite this article

M. Abd Ellateif T. and Maitra S. Some studies on the surface modification of sol-gel derived hydrophilic Silica nanoparticles. Int. J. Nano Dimens., 2017; 8(2): 97-106., DOI: 10.22034/ijnd.2017.25013

INTRODUCTION

Nanoparticles (NPs) with effective size range from 1-100 nm have attracted significant interests among the researchers due to their unique properties like, very large surface area, highly active surface sites. These properties enable the NPs suitable for a wide range of applications in the areas of membrane, catalysis, sorption of metal ions, enzyme encapsulation, drug delivery etc. [1, 2]. Silica NPs occupy an important position in this regard because of the ease in its preparation and their wide range of usage in various industrial applications, such as catalysis, adsorption, pigments, pharmacy, electronic sensors as well as in different biotechnological applications exploiting there several unique characteristics like, high surface area, porosity as well as thermal, chemical and mechanical stability [3, 4].

Silica nanoparticles can be prepared by three main processes: reverse micro-emulsion, flame synthesis and the widely utilized Stober sol-gel method [5-7]. Both reverse micro-emulsion and sol-gel methods are based on the hydrolysis and condensation of tetraethyl orthosilicate (TEOS) and tetramethyl orthosilicate (TMOS) under acidic or basic conditions [8]. The synthesized silica nanoparticles using these two methods have spherical shapes with smooth surfaces covered by hydroxyl groups [6, 9].

Sol gel method follows a soft-chemistry route to produce oxide and hybrid materials with controlled properties like, chemical composition, microstructure, morphology and surface functionalization [10]. It involves a two-step reaction, hydrolysis of a metal alkoxide ($Si(OR)_4$) such as tetraethylorthosilicate (TEOS, $Si(OC_2H_5)_4$) or inorganic salts such as sodium silicate (Na_2SiO_3) in the presence of mineral acid (e.g., HCl) or base (e.g., NH_3) as catalyst [7, 11, 12], followed by its condensation [6, 7, 13, 14].

The reactions of TEOS towards the formation of silica particles in the sol-gel process are written

* Corresponding Author Email: Tayseir07@yahoo.com

as in equations (1-3) [7, 15-17]. The first reaction is the hydrolysis of TEOS molecules that form silanol groups. The condensation/polymerization between the silanol groups (reaction 2) or between silanol groups and ethoxy groups (reaction 3) creates siloxane bridges (Si–O–Si) that form the entire silica structure.

$$Si(OC_2H_5)_4 + H_2O \xrightarrow{\text{hydrolysis}} Si(OC_2H_5)_3OH + C_2H_5OH \quad (1)$$

$$\equiv Si-O-H + H-O-Si \equiv \xrightarrow{\text{watercondensation}} \equiv Si-O-Si \equiv + H_2O \quad (2)$$

$$\equiv Si-OC_2H_5 + H-O-Si \equiv \xrightarrow{\text{alcohol condensation}} \equiv Si-O-Si \equiv + C_2H_5OH \quad (3)$$

Due to the high surface energy and abundant hydroxyl groups (Silanol-Si-OH) on the silica surface, Silica NPs tend to agglomerate. It results in the development of an affinity with the polymer matrix which makes them hydrophilic [18, 19]. Therefore, a modification in the synthesis process to develop a hydrophobic surface is necessary for improving the dispersion and compatibility of nano-silica particles in an organic matrix [20-22]. This modification can be achieved through the reaction between the silanol groups and various reagents to render the silica hydrophobic [23, 24]. Thus, a critical factor in the design of surface-modified NPs is the controlled attachment of a desired functional group onto the surface of the NPs [25-27].

Alumino silicate (Al_2O_3-SiO_2) system have extensively studied by the researchers for the potential usages of these mixed oxides as catalyst supports [28]. They are of particular interest in heterogeneous catalysis because of their acid and basic properties that can strongly affect the activity and selectivity of the final catalyst [29]. Different approaches have been used in the preparation of alumino silicates which include co-precipitation, hydrothermal processing, chemical vapour deposition (CVD) and colloidal and polymeric sol gel methods, with the aim of producing homogeneous mixtures with desired phases at a comparatively lower temperature. Corma and Pariente [30] have synthesized amorphous silica- alumina by a conventional co-gel procedure using tetra alkylammonium ions as compensating cations. It was done with the objective of retaining most of the aluminum in the tetrahedral position thereby controlling the pore size, thermal stability and density of the acid sites. Overall, the sol gel process has been shown to be particularly effective in producing the materials that satisfy this aim [28].

In this study, we have synthesized silica NPs using sol gel method. To modify the hydrophilic surface of silica NPS to hydrophobic one alumina sol was used to produce silica-alumina nanoparticles. The hydrophobic nature of these nanoparticles has been controlled by changing the proportions of the modifier. This work provides new insights into the modification of silica surface for advanced applications of the silica-based nanomaterials where the hydrophobic nature of the material is well desired.

EXPERIMENTAL

Materials

Chemicals used in this work to synthesize silica and aluminum sols were: Tetraethoxy orthosilicate (TEOS) of 98 v.% purity and aluminum isopropoxide 98 v.% purity and were purchased from Acros Organics. Ethanol with a purity of 95 v.%. was received from HMbG Chemicals. Ammonia and nitric acid of 29 v.% and 65 v.% assay respectively were both obtained from R & M Chemicals. All starting materials were used as received without further purification.

Synthesis of Silica Sols

TEOS was used as the starting material for the synthesis of silica sol. The hydrolysis reaction of TEOS was performed under base catalyzed conditions using ammonia. The molar ratios between the different precursors, namely, TEOS, NH_3 and H_2O were 0.5:0.5:10 respectively. The hydrolysis reaction of TEOS through the addition of water (Eq. 1) replaces its alkoxide groups (OC_2H_5) with hydroxyl groups (OH^-). Subsequently, water condensation reaction (Eq. 2) and alcohol condensation (Eq. 3) of the silanol groups (Si-OH) produced siloxane bonds (Si-O-Si) [7, 15-17].

Synthesis of Alumina Sols

To synthesize alumina sol, alumina isopropoxide (8.17 g) was dissolved in 72 ml deionized water following the procedure described by Buelna [31]. The solution mixture was then heated at 80°C for 20 min and to it 126 ml nitric acid was added. The mixture was then covered with aluminum foil and kept in the oven at 95°C for 24 h.

Surface modification of silica sols

Alumina sols in three different proportions (1, 3 and 5 %) were added to the respective silica sols. The hydrophilic silica was then converted to hydrophobic materials following Eq. 4 as illustrated in Fig. 2. The synthesized sols were kept at room temperature for 24 h, dried at 105°C, followed by grinding to a fineness of -60 mesh. The change in hydrophobicity of silica nanoparticles as a consequence of doping has been presented by the schematics given below (Fig. 1 and Fig. 2 drawn by Chem Sketch software).

$$Si - OH + Al_2O_3 \rightarrow \equiv Si - O - Al = + H_2O \quad (4)$$

Characterization techniques

To characterize the synthesized silica NPs (unmodified and modified) different techniques were used. The modified synthesized silica NPs were characterized using FTIR spectrophotometer (Shimadzu FTIR-8400S) and XRF (4kW S4 PIONEER X-ray spectrometer). The nanoparticle morphology was analyzed using FESEM (Zeiss, SUPRA 55VP), and particle size and particle distribution using TEM (Zeiss, Libra 200). The surface area of the synthesized nanoparticles was measured using surface area and pore size analyzer (Micromeritics ASAP 2000). Additionally the thermal stability was studied using TGA (Perkin-Elmer, Pyris V-3.81).

RESULTS AND DISCUSSION

FTIR spectra of the synthesized silica nanoparticles

The Fourier transform infrared spectroscopy (FTIR) of the synthesized silica NPs before and after surface modification is shown in Fig. 3. The peaks at 3400 Cm^{-1} and at 1650 Cm^{-1} correspond to the stretching vibration of OH^- and C-H groups from organic part of the precursor, respectively. The main peak at 1000–1250 Cm^{-1} was attributed to the stretching vibration modes of Si-O-Si bridging (Fig. 3a). The peak at 981 Cm^{-1} (Fig. 3b, 3c and 3d) was attributed to the presence of Si-O-Al stretching vibration indicating the modification of silica surface. The obtained FTIR results for the synthesized silica are matching well to those reported in the literature [32, 33].

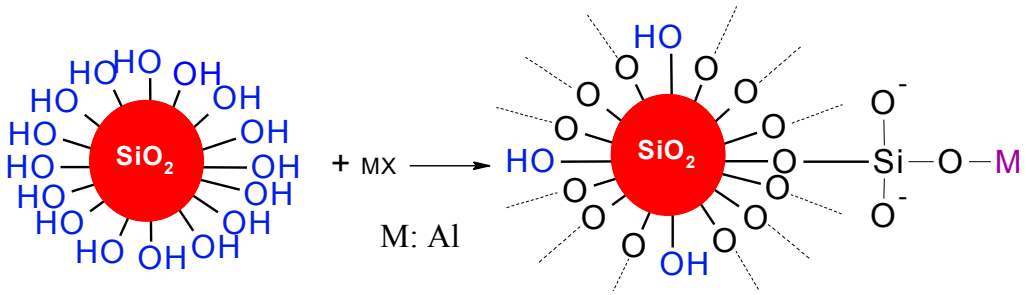

Fig. 1: Surface modification step of silica.

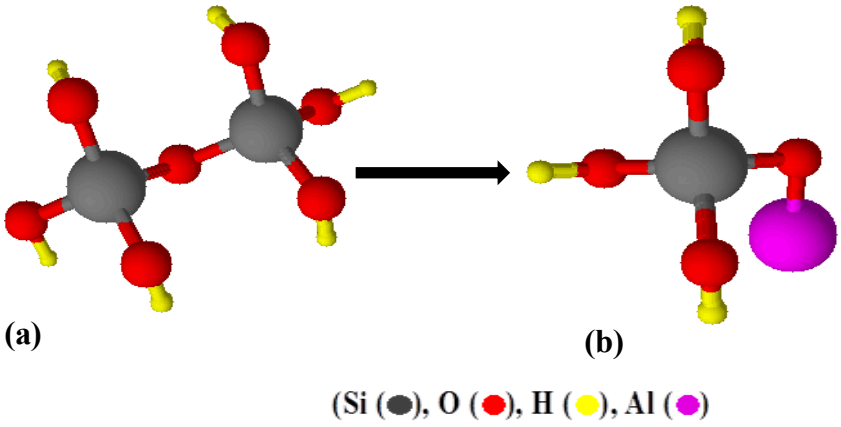

Fig. 2: The structure of the synthesized (a) unmodified silica (b) silica alumina.

XRF of the synthesized silica nanoparticles

Elemental composition of the modified and unmodified silica nanoparticles was determined by XRF analysis. The results have been presented in Fig. 4. It shows that oxygen and silica were present predominantly while alumina was present in trace amounts. The proportion of alumina increased with the increase in the proportions of alumina modifier.

Hydrophobicity of the synthesized silica nanoparticles

During its drying, the reaction between OH-groups at the surface of silica NPs results in the formation of alkoxysilane groups to develop hydrophobicity in silica [34, 35]. Both, unmodified and modified silica NPs were tested for hydrophilicity. They were exposed to atmospheric moisture at a temperature of 25°C and their water adsorption was measured from the gain in weight of the samples [36]. Fig. 5 shows the weight gain of unmodified silica compared to that of silica modified using alumina. The gain in weight of unmodified silica was about 8% which was obtained over a period of 60 days. In the other hand, the silica modified with 1, 3 and 5 % alumina showed a gain in weight of 5, 2 and 1 %, respectively. It indicates that alumina addition has a profound influence in reducing the hydrophilicity of the synthesized silica nanoparticles.

FESEM micrographs of the synthesized silica nanoparticles

The micrographs of unmodified and modified silica nanoparticles with different proportion of alumina were characterized using FESEM with 2000 KX magnifications for studying the morphology of silica NPs as a result of alumina addition. The unmodified silica NPs (Fig. 6a) showed very fine particles with smooth surface and low packing density compared to the morphology of silica alumina NPs (Fig. 6b, 6c and 6d). Silica NPs exhibited differences in the morphology depending on the percentage of alumina. The lowest packing density of the particles was obtained for the silica modified with 1% alumina with spherical alumina particles cover the surface of silica NPs. However, with the increase in the proportion of alumina to 3% and 5%, the morphology of silica NPs appeared to be denser and monolithic.

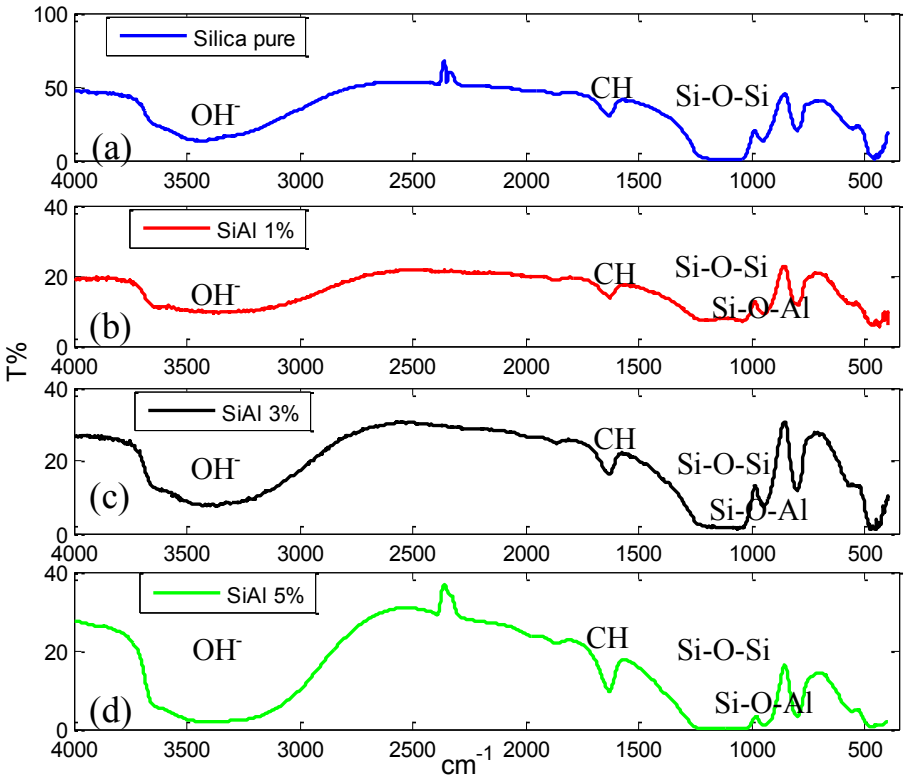

Fig. 3: FTIR of (a) unmodified silica (b) silica alumina 1% (c) silica alumina 3% (d) silica alumina 5%.

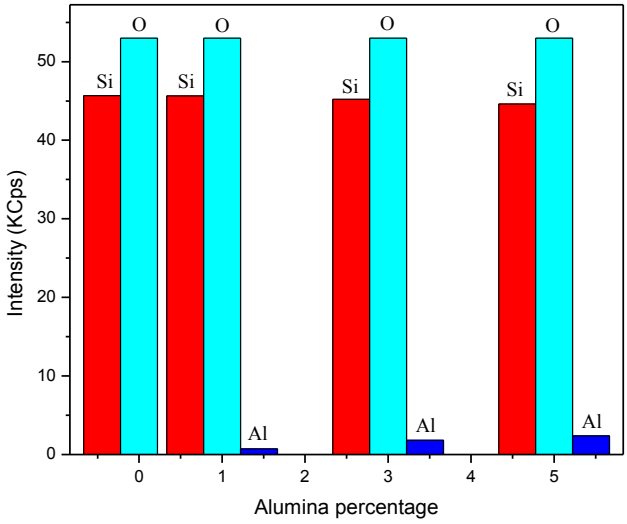

Fig. 4: Pure silica and silica alumina nanoparticles XRF results.

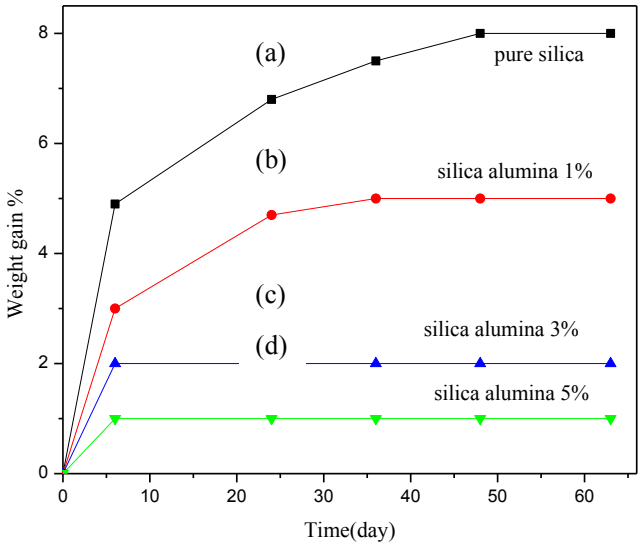

Fig. 5: Weight gain of the (a) unmodified silica nanoparticles (b) silica alumina 1% (c) silica alumina 3% (d) silica alumina 5%.

TEM particle distribution of the synthesized silica nanoparticles

The particle distribution of unmodified silica and modified silica NPs with different proportions of alumina was investigated using TEM as shown in Fig. 6. The unmodified silica nanoparticles agglomerated together with a particle size of 35 nm (Fig. 6e) while the particle distribution of modified silica nanoparticle illustrated small sized silica NPs (12 nm) agglomerate around the relatively larger particles of alumina (125 nm) replacing the hydroxyl group at silica surface [6]. For silica nanoparticles modified with 1% alumina (Fig. 6f), alumina particles were distributed at the surface of silica. With the increase in the proportion of alumina to 3%, the silica NPs cover the surface of alumina and agglomerated around alumina particles resulting in rough surface (Fig. 6g). The micrograph of silica with 5% alumina (Fig. 6h) illustrated branch structure of silica NPs and agglomeration around alumina particles. The morphological variation is likely to have a significant influence on the properties like surface area and porosity.

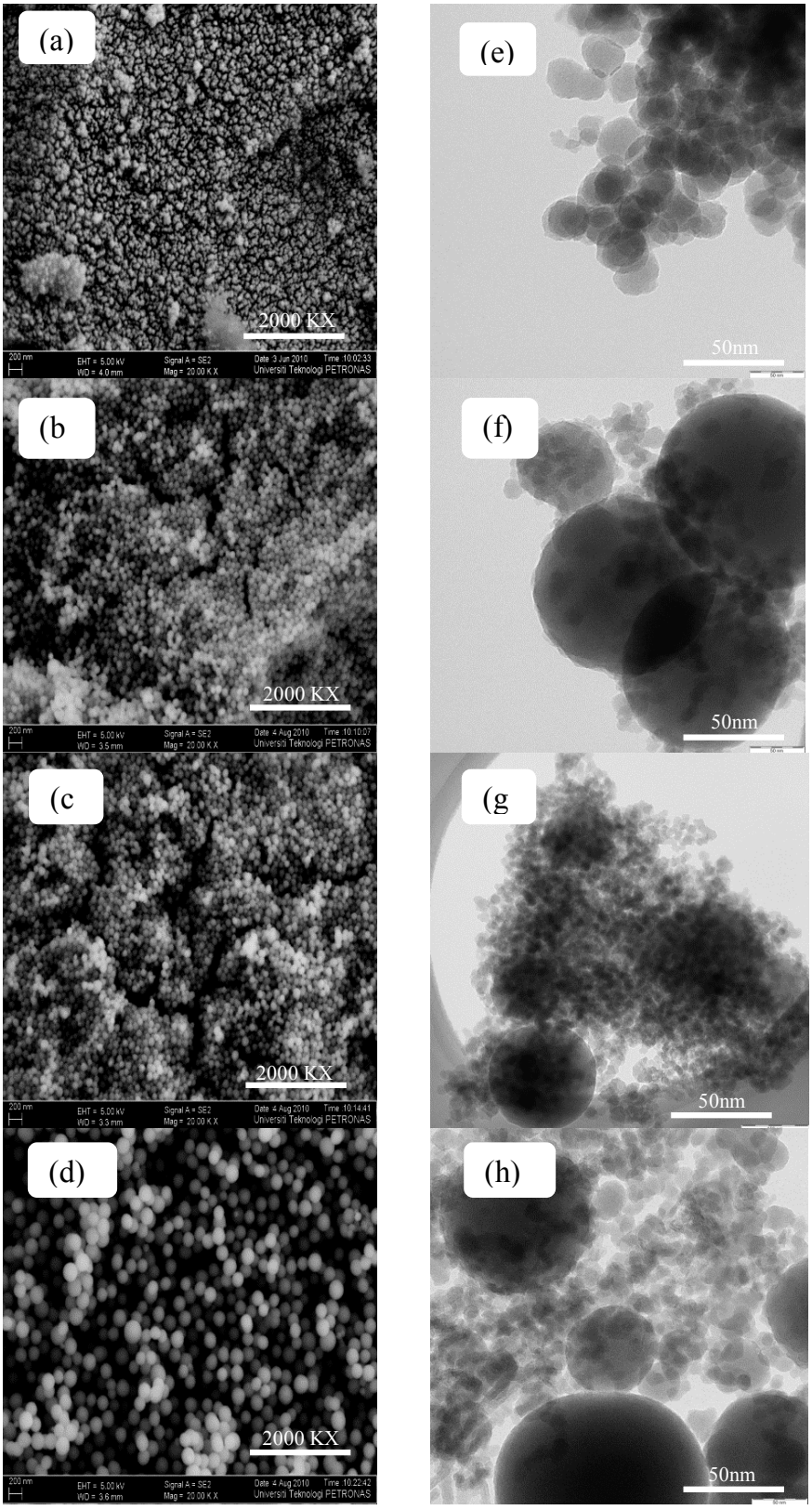

Fig. 6: FESEM of the (a) unmodified silica nanoparticles (b) silica alumina 1% (c) silica alumina 3% (d) silica alumina 5% and TEM of the (e) unmodified silica nanoparticles (f) silica alumina 1% (g) silica alumina 3% (h) silica alumina 5%.

BET of the synthesized silica nanoparticles

The nitrogen adsorption-desorption isotherms of the synthesized unmodified and modified silica NPs with different percentage of alumina have been presented in Fig. 7. It can be seen that all the samples showed type (V) hysteresis according to BET classification, indicating the presence of mesopores (2–50 nm). Further studies indicated that with the increase in the modifier (Fig. 7), the hysteresis loops shifted to higher relative pressure range and the areas of the hysteresis loops decreased. This indicated that the average pore size increased and the volume of pore decreased with the increase in the proportion of the modifiers. The estimated surface area and the pore size of unmodified and modified silica NPs were investigated using the BET equation. The surface area of unmodified silica NPs was relatively high (303 m^2/g) due to the presence of small sized pores (4.36 nm) as shown in Table 1. With the modification of silica with alumina the surface area reduced depending on the particle size distribution as shown in FESEM and TEM results. Silica nanoparticles modified with 1% alumina develops surface area of 119 m^2/g with pore size of 8.13 nm. The surface area was relatively high for silica modified with 3% alumina (165 m^2/g), due to the distribution of silica NPs at the surface of alumina leading to the development of rough surface and small sized pores (6.89 nm). Silica with 5% alumina resulted in a decrease in the surface area and increase in the pore size (121 m^2/g, 9.91 nm). This can be related to the presence of large amounts of alumina particles at the surface of silica NPs. With the increase in alumina content the pore volume changed from 0.24, 0.3 and 0.28 cm^3/g due to silica nanoparticles different distribution at the surface as mentioned earlier in the TEM micrograph. The small pore size of the synthesized silica changed from 4.3 nm to 9.9 nm indicating a mesoporous structure (2-50 nm) of the synthesized silica which was in agreement with N_2 adsorption-desorption type (V) plot shown in Fig. 7.

Thermal stability of the synthesized silica nanoparticles (TGA)

The physically adsorbed water and hydroxyl group content of NPS were evaluated quantitatively by TGA (Fig. 8). The TGA graphs of the synthesized silica and silica alumina particles were divided into three different regions a) the first part from 0 to 100°C corresponded to gas desorption; b) the second regime from 100 to 400°C corresponded to physical desorption of adsorbed water and; c) the third regime from 400 to 800°C corresponded to dehydroxylation of adjacent –OH groups on the surface.

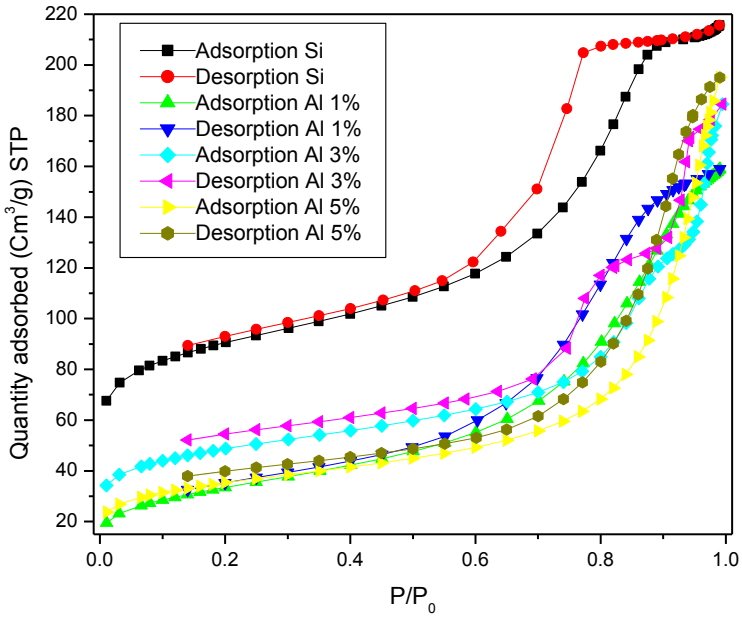

Fig. 7: N_2 adsorption-desorption isotherms of the unmodified silica nanoparticles and silica alumina 1%, silica alumina 3% and silica alumina 5%.

Table 1: Surface area of the synthesized silica nanoparticles.

Sample	Surface are (m^2/g)	Pore size (nm)	Pore volume (cm^3/g)
Pure silica	303.69	4.36	0.33
1% Al_2O_3	119.74	8.13	0.24
3% Al_2O_3	165.67	6.89	0.30
5% Al_2O_3	121.69	9.91	0.28

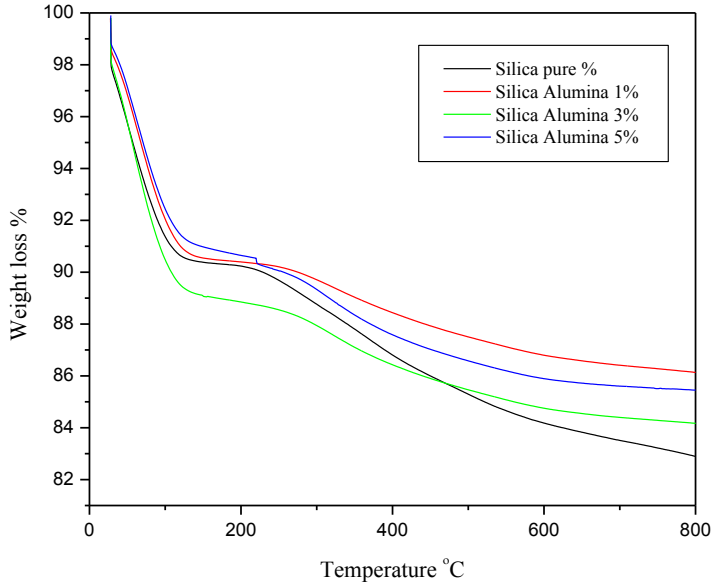

Fig. 8: Thermal stability (TGA) of the synthesized pure silica and silica alumina nanoparticles.

The weight loss for silica NPs modified with 1% alumina was lower than that of pure silica NPs. It was related to the presence of alumina particles replacing the hydroxyl group at the surface of silica. Higher weight loss was noted for 3% alumina NPs due to the presence of excess silica at the surface (as shown in TEM results, Fig. 6). The initial 11% weight loss observed between 0°C and 100°C was related to the absorbed water and moisture loss in the sample. The subsequent 14% loss in weight observed between 100°C and 400°C were related to the loss of strongly bonded water molecules. Lower weight loss was observed for silica with 5% alumina with initial 9% loss between 0 and 100°C. It represented absorbed water and moisture in the sample. The following 12% weight loss in the sample, occurring between 100 and 400°C was explained by the loss of strongly bonded water molecules (hydrogen bonded). The weight loss of the synthesized silica alumina particles was dependent on the particle size distribution of the samples. It has also been noticed that the three mass loss regimes overlapped considerably with each other. Hence, the exact water content and densities of hydroxyl groups could not be determined easily and exactly. The obtained results were in good agreement with the literature data [37].

CONCLUSION

Modification of silica NPs with different proportions of alumina was carried out by sol-gel method. The characteristics of the synthesized silica alumina nanoparticles and the influence of added alumina percentage on the texture of silica were investigated by FTIR, XRF, FESEM, TEM, BET and TGA studies. FTIR and XRF results confirmed the synthesis and modification of silica nanoparticles. The proportions of modification resulted in a marked influence on the morphology and particle size distribution. The nitrogen adsorption–desorption isotherms showed a type (V) adsorption isotherm indicating the mesoporous nature of the synthesized silica alumina with a

reduction in the surface area compared to the unmodified silica NPs. The TGA results indicated high thermal stability of the synthesized materials up to 800°C. The weight losses observed at 100°C and 400°C were attributed to the loss of physically absorbed moisture and chemically bonded water. The hydrophilicity tests of both unmodified and modified silica NPs showed a decrease in the weight gain from 8% for unmodified NPs to a minimum gain of 1% obtained for modified NPs with 5% alumina. The modified silica with 1, 3 and 5% alumina showed weight gains of 5, 2 and 1%, respectively, over the entire period demonstrating a direct relationship between the proportion of alumina and the hydrophilicity of the synthesized silica NPs.

CONFLICT OF INTEREST

The authors declare that there is no conflict of interests regarding the publication of this manuscript.

REFERENCES

[1] Hwang T., Lee H., Kim H., Kim G., (2010), Two layered silica protective film made by a spray-and-dip coating method on 304 stainless steel. *J. Sol-Gel sci. Technol.* 2010: 1-6.

[2] Oh Y., Hong L., Asthana Y., Kim D., (2006), Synthesis of super-hydrophilic mesoporous silica via a sulfonation route. *J. Indus. Engineer. Chem.* 12: 911-917.

[3] Barandeh F., Nguyen P., Kumar R., Iacobucci G., Kuznicki M., Kosterman A., Bergey E., Prasad P., Gunawardena S., (2012), Organically modified silica nanoparticles are biocompatible and can be targeted to neurons in vivo. *PLoS ONE.* 7: 1-15.

[4] Ramazani A., Farshadi A., Mahyari A., Sadri F., Joo S., Azimzadeh Asiabi P., Taghavi Fardood S., Dayyani N., Ahankar H., (2016), Synthesis of electron-poor N-Vinylimidazole derivatives catalyzed by Silica nanoparticles under solvent-free conditions. *Int. J. Nano Dimens.* 7: 41-48.

[5] Lin Y., (2001), Microporous and dense inorganic membrane: Current status and prospective. *Sep. Purif. Technol.* 25: 39-55.

[6] Zou H., Shen S., (2008), Polymer/silica nanocomposites: Preparation, characterization, properties, and application. *Chem. Rev.* 108: 3893-3957.

[7] Hench L., (1990), The sol-gel process. *Chem. Rev.* 90: 33-72.

[8] Brinker C., (1988), Hydrolysis and condensation of silicates: Effects on structure. *J. Non-Cryst. Solids.* 100: 31-50.

[9] Xu S., Hartvickson S., Zhao J., (2011), Increasing surface area of silica nanoparticles with a rough surface. *ACS Appl. Mater. Interfaces.* 3: 1865-1872.

[10] Falcaro P., Innocenzi P., (2009), X-rays to study, induce, and pattern structures in sol–gel materials. *J. Sol-Gel Sci. Technol.* 57: 236-244.

[11] Klabunde K., Stark J., Koper O., Mohs C., Park D., Decker S., Jiang Y., Lagadic I., Zhang D., (1996), Nanocrystals as stoichiometric reagents with unique surface chemistry. *J. Phys. Chem.* 100: 12142-12153.

[12] Stöber W., Fink A., Bohn E., (1968), Controlled growth of monodisperse silica spheres in the micron size range. *J. Colloid Interface Sci.* 26: 62-69.

[13] Prabakar S., Assink R., (1997), Hydrolysis and condensation kinetics of two component organically modified silica sols. *J. Non-Cryst. Solids.* 211: 39-48.

[14] Zhang X., Zhao S., Gao C., Wang S., (2009), Amorphous sol–gel SiO_2 film for protection of an orthorhombic phase alloy against high temperature oxidation. *J. Sol-Gel Sci. Technol.* 49: 221-227.

[15] Brinker C., Scherer G., Sol-gel science: The physics and chemistry of sol-gel processing: Academic Pr, 1990.

[16] Silva C., Airoldi C., (1997), Acid and base catalysts in the hybrid silica sol-gel process. *J. Colloid Interface Sci.* 195: 381-387.

[17] Brinker C., Scherer G., (1990), The physics and chemistry of sol-gel processing. *J. Sol-Gel Sci. Technol.* 141: 58-59.

[18] Jesionowski T., Krysztafkiewicz A., (1999), Properties of highly dispersed silicas precipitated in an organic medium. *J. Dispersion Sci. Technol.* 20: 1609-1623.

[19] An D., Wang Z., Zhao X., Liu Y., Guo Y., Ren S., (2010), A new route to synthesis of surface hydrophobic silica with long-chain alcohols in water phase. *Colloids and Surf. A: Physicochem. Engineer. Aspects.* 369: 218-222.

[20] Dékány I., Szántó F., Nagy L., (1985), Sorption and immersional wetting on clay minerals having modified surface. I. Surface properties of nonswelling clay mineral organocomplexes. *J. Colloid Interface Sci.* 103: 321-331.

[21] Vrancken K., Possemiers K., Van Der Voort P., Vansant E., (1995), Surface modification of silica gels with aminoorganosilanes. *Colloids and Surf. A: Physicochem. Engineer. Aspects.* 98: 235-241.

[22] Daniels M., Francis L., (1998), Silane adsorption behavior, microstructure and properties of glycidoxypropyltrimethoxysilane-modified colloidal silica coatings. *J. Colloid Interface Sci.* 205: 191-200.

[23] Xie Y., Hill C., Xiao Z., Militz H., Mai C., (2010), Silane coupling agents used for natural fiber/polymer composites: A review. *Composites Part A.* 41: 806-819.

[24] Kaas R., Kardos J., (1971), Interaction of alkoxy silane coupling agents with silica surfaces. *Polym. Eng. Sci.* 11: 11-18.

[25] Aissaoui N., Bergaoui L., Landoulsi J., Lambert J., Boujday S., (2012), Silane layers on silicon surfaces: Mechanism of interaction, stability and influence on protein adsorption. *Langmuir*.28: 656-665.

[26] Simon A., Cohen-Bouhacina T., Porté M., Aimé J., Baquey C., (2002), Study of two grafting methods for obtaining a 3-Aminopropyltriethoxysilane monolayer on silica surface. *J. Colloid Interface Sci.* 251: 278-283.

[27] Howarter J., Youngblood J., (2006), Optimization of silica silanization by 3-Aminopropyltriethoxysilane. *Langmuir.* 22: 11142-11147.

[28] Nampi P., Moothetty P., Berry F., Mortimer M., Warrier K., (2010), Aluminosilicates with varying alumina-silica ratios: Synthesis via a hybrid sol-gel route and structural characterisation. *Dalton Transactions.* 39: 5101-5107.

[29] Cónsul J., Costilla I., Gigola C., Baibich I., (2008), NO reduction with CO on alumina-modified silica-supported palladium and molybdenum-palladium catalysts. *Appl. Catal. A.* 339: 151-158.

[30] Corma A., Pérez-Pariente J., Fornés V., Rey F., Rawlence D., (1990), Synthesis and characterization of silica-alumina prepared from tetraalkylammonium hydroxides. *Appl. Catal.* 63: 145-164.

[31] Buelna G., (1999), Sol-gel-derived mesoporous [gamma]-

alumina granules. *Microporous Mesoporous Mater.* 30: 359-369.

[32] May M., Asomoza M., Lopez T., Gomez R., (1997), Precursor aluminum effect in the synthesis of sol- gel Si- Al Catalysts: FTIR and NMR characterization. *Chem. Mater.* 9: 2395-2399.

[33] Cheng Z., Yang Y., (2008), Synthesis and characterization of aluminum particles coated with uniform silica shell. *Transact. Nonferrous Metals Soc. of China.* 18: 378-382.

[34] Rao A., and Wagh P., (1998), Preparation and characterization of hydrophobic silica aerogels. *Mater. chem. phys.* 53: 13-18.

[35] Wagh P., Rao A., Haranath D., (1998), Influence of molar ratios of precursor, solvent and water on physical properties of citric acid catalyzed TEOS silica aerogels. *Mater. chem. phys.* 53: 41-47.

[36] Reynolds J., Coronado P., Hrubesh L., (2001), Hydrophobic aerogels for oil-spill clean up-synthesis and characterization. *J. Non-Cryst. Solids.* 292: 127-137.

[37] Song He A. Z., Xiaojing Shi A., Hui Yang A., Lunlun Gong A., Xudong Ch., (2015), Rapid synthesis of sodium silicate based hydrophobic silica aerogel granules with large surface area. *Adv. Powder Technol.* 26: 537-541.